



Published in final edited form as:

Eur J Radiol. 2015 September ; 84(9): 1685–1693. doi:10.1016/j.ejrad.2015.03.016.

Ultrasound Molecular Imaging: Moving Towards Clinical Translation

Lotfi Abou-Elkacem, PhD[#], Sunitha V. Bachawal, PhD[#], and Jürgen K. Willmann, MD

Department of Radiology, Molecular Imaging Program at Stanford, Stanford University, School of Medicine, Stanford, California, USA

Abstract

Ultrasound is a widely available, cost-effective, real-time, non-invasive and safe imaging modality widely used in the clinic for anatomical and functional imaging. With the introduction of novel molecularly-targeted ultrasound contrast agents, another dimension of ultrasound has become a reality: diagnosing and monitoring pathological processes at the molecular level. Most commonly used ultrasound molecular imaging contrast agents are micron sized, gas-containing microbubbles functionalized to recognize and attach to molecules expressed on inflamed or angiogenic vascular endothelial cells. There are several potential clinical applications currently being explored including earlier detection, molecular profiling, and monitoring of cancer, as well as visualization of ischemic memory in transient myocardial ischemia, monitoring of disease activity in inflammatory bowel disease, and assessment of arteriosclerosis. Recently, a first clinical grade ultrasound contrast agent (BR55), targeted at a molecule expressed in neoangiogenesis (vascular endothelial growth factor receptor type 2; VEGFR2) has been introduced and safety and feasibility of VEGFR2-targeted ultrasound imaging is being explored in first inhuman clinical trials in various cancer types. This review describes the design of ultrasound molecular imaging contrast agents, imaging techniques, and potential future clinical applications of ultrasound molecular imaging.

Keywords

Molecular Imaging; microbubbles; ultrasound; cancer; inflammation; clinical translation

INTRODUCTION

Ultrasound is the second most commonly used imaging technique in the clinic. It is noninvasive, widely available, portable, relatively inexpensive and allows real-time imaging without the use of ionizing radiation [1–3]. In recent years, ultrasound has emerged into a

Corresponding author, Jürgen K. Willmann, M.D., Department of Radiology, Molecular Imaging Program at Stanford, School of Medicine, Stanford University, 300 Pasteur Drive, Room H1307, Stanford, CA 94305-5621, P: 650-723-5424; Fax: 650-723-1909, willmann@stanford.edu.

[#]Equal contribution

Publisher's Disclaimer: This is a PDF file of an unedited manuscript that has been accepted for publication. As a service to our customers we are providing this early version of the manuscript. The manuscript will undergo copyediting, typesetting, and review of the resulting proof before it is published in its final citable form. Please note that during the production process errors may be discovered which could affect the content, and all legal disclaimers that apply to the journal pertain.

molecular imaging technique through the introduction of novel, molecularly-targeted contrast agents that can visualize disease processes at the molecular level by accumulating at tissue sites overexpressing certain molecular markers. Currently, most widely used molecular ultrasound contrast agents are micron sized gas bubbles that are composed of an insoluble gas stabilized by a shell. Due to their size of several micrometers, microbubbles remain within the vascular compartment and are therefore particularly well suited for detecting and monitoring disease processes that are characterized by a differential expression of molecules on the vasculature, such as many types of cancer or inflammatory diseases [4]. Multiple preclinical studies have shown that molecular imaging with ultrasound is safe and accurate and several research groups are currently translating various ultrasound molecular imaging concepts from small to large animal models of human diseases. Recently, a first clinical grade ultrasound molecular imaging contrast agent has entered clinical trials to visualize expression levels of a molecular marker expressed in neoangiogenesis of cancer (vascular endothelial growth factor receptor type 2; VEGFR2).

In this review, we describe the design of ultrasound molecular imaging contrast agents, imaging techniques, and potential future clinical applications of ultrasound molecular imaging.

Design and Biodistribution of Molecularly-Targeted Microbubbles

The best studied and most commonly used ultrasound molecular imaging contrast agents are microbubbles. Microbubbles, usually ranging in size between 1 and 4 μm , consist of a gas core stabilized by a surrounding shell [4]. The shell can consist of various materials such as phospholipids, biocompatible polymers, or proteins. These compounds are used to stabilize microbubbles and to reduce gas dissolution in blood (Figure 1). Various gas types have been used as gas cores including room air, nitrogen, or heavy, biologically inert gases such as perfluoropropane, perfluorobutane, perfluorohexane, or sulfur hexafluoride [5]. In comparison to room air, heavy gases are poorly soluble in water or blood and, thus, dissolve at a slower rate into the surrounding solution. Therefore, heavy gases facilitate better stability with a longer blood half-life of the microbubbles. For details on the chemical synthesis of microbubbles please refer to previous review articles [4, 5].

In general, there is no significant difference in the process of synthesizing non-targeted versus molecularly targeted microbubbles. However, designing molecularly-targeted contrast microbubbles also involves a process which adds binding ligands to the shell of the microbubbles to make them accumulate at tissue sites expressing the molecules at which the agents are targeted. The targeting ligand can be antibodies, peptides, or natural or engineered scaffolds and can be either directly incorporated into the shell during or after microbubble synthesis or to a distal end of poly-ethylene-glycol (PEG) chains (Figure 1).

Recently, a first clinical grade molecular ultrasound contrast agent has been designed [6] which has entered first in-human clinical trials [7]. This contrast agent, also called BR55 (Bracco, *** Italy), consists of a gas core (mixture of perfluorobutane and nitrogen), surrounded by a phospholipid shell with a mean diameter of 1.5 μm [6, 8]. The heterodimeric peptide binding ligand is targeted at kinase insert domain receptor (KDR; the human analog of vascular endothelial growth factor receptor type 2; VEGFR2). VEGFR2 is

overexpressed on the neovasculature of many human cancer types including prostate cancer, breast cancer, ovarian cancer, pancreatic cancer, and colorectal cancer to mention just a few (Table 1).

Following intravenous injection, microbubbles are rapidly cleared from the circulation primarily through the RES. The gas is exhaled and the shell enters the phospholipid pool in the body. Early studies on the biodistribution of non-targeted microbubbles using air filled serum albumin microbubbles radiolabelled with Iodine-123 showed that the gas from the microbubbles can be measured in the exhalation air within minutes [9]. Using radiolabeling and dynamic whole-body micro-PET imaging in tumor-bearing mice it has been shown that molecularly-targeted microbubbles are also rapidly cleared from the blood stream with a half-life of 3.5 minutes [10]. The vast majority of microbubbles are cleared by the hepatic and splenic reticuloendothelial system (RES) with 95% of the microbubbles cleared from the blood pool after 30 minutes [10].

Since the background signal from freely circulating targeted microbubbles rapidly decreases, ultrasound molecular imaging can be performed a few minutes following intravenous administration of the imaging probe. This is a major advantage compared to other molecular imaging techniques such as Positron Emission Tomography (PET) or Single Photon Emission Computed Tomography (SPECT) usually requiring at least one hour or longer waiting times between injection and data acquisition, depending on the radionuclide and radiotracer used [11]. This unique *in vivo* biodistribution with rapid clearance also allows repetitive injections of targeted microbubbles as needed, for example to scrutinize a certain anatomical area several times or to extend the area examined with ultrasound molecular imaging within the same imaging session.

Detection of Ultrasound Molecular Imaging Signal

A prerequisite of ultrasound molecular imaging is the sensitive differentiation of imaging signal from molecularly attached microbubbles compared to background signal. Low mechanical index (MI) imaging (MI of 0.1 or less) allows visualization of microbubbles without destroying them. Acoustic waves with alternating positive and negative pressures compress the microbubble with the positive pressure, and expand it with the negative pressure, causing periodic changes of its radius [12]. During the phase of compression and expansion, microbubbles generate asymmetric nonlinear oscillations, vibrations and alterations in acoustic impedance which strongly depend on the microbubble radius. These asymmetric nonlinear oscillations result in the generation of harmonic (second harmonics and above) or subharmonic (half of the center frequency) echoes which can be leveraged to enhance the signal to noise from attached microbubbles compared to the surrounding tissue using various contrast imaging technologies (such as Pulse Inversion or Amplitude Modulation) which are reviewed elsewhere [4]. Using these techniques, ultrasound molecular imaging is one of the most sensitive molecular imaging modalities that potentially allows depicting a single microbubble, as shown in a phantom study [12], implying picogram sensitivity.

Quantification of Ultrasound Molecular Imaging Signal

Ultrasound molecular imaging uses the same contrast imaging technologies already implemented on clinical ultrasound systems for non-targeted contrast-enhanced ultrasound imaging as described above. In contrast to non-targeted ultrasound imaging, in ultrasound molecular imaging the signal from a small amount of molecularly attached microbubbles needs to be separated from signal attributed to freely circulating, non-attached microbubbles [4], assuming that only a small fraction (1% or less) of the injected targeted microbubble dose actually binds to the molecular targets [10]. Several approaches have been explored to reliably measure ultrasound molecular imaging signal. One approach includes a waiting time of about 10 min following contrast injection to allow most of the freely circulating microbubbles to be cleared from the blood circulation; this is followed by ultrasound data acquisition attributed primarily to attached microbubbles [6]. While this approach is straight forward and allows qualitative assessment if high enough numbers of contrast agents attach to the molecular target, it is not suited for quantitative assessment or longitudinal monitoring of molecular imaging signals since at the time of data acquisition some of the attached microbubbles might have been degraded and the measured imaging signal is confounded by still freely circulating microbubbles.

A more quantitative approach is called destruction-replenishment method which allows separation of the imaging signal from targeted and freely circulating microbubbles and which is commonly used in preclinical experiments. Here, the difference in imaging signal measured pre and post microbubble destruction corresponds to the molecularly-targeted ultrasound imaging signal (Figure 2) [13]. In addition to reporting absolute values obtained from calculating the difference in imaging signal, the ratio of imaging signal pre and post destruction can be used as a value which is independent of tissue attenuation and system settings, which becomes important when translating the technique from small to large animal experiments and eventually to patients where tissue attenuation can vary substantially depending on body habitus and location of the imaging area within the body [14]. However, the main disadvantages are the required time-consuming post-processing, hampering the real-time work flow of ultrasound imaging and the fact that microbubbles need to be destroyed, which by itself can have unwarranted biological consequences caused by microbubble-induced cavitation [15, 16].

Ongoing research explores faster and more real-time and clinically translatable data quantification approaches without the need of a destructive pulse. One concept is based on a threshold-determined “dwell time” measurement of microbubbles obtained in each imaging voxel, thereby allowing differentiation of stationary (attached) from circulating microbubble signals and which has been shown to correlate well compared with the aforementioned destruction replenishment approach [17]. Recently a new concept of signal quantification using acoustic radiation force (ARF) has been introduced (Figure 2). In this approach, a “residual-to-saturation” ratio (which is the ratio of imaging signal with and without the ARF push pulse) is measured which is a quantitative parameter independent of ultrasound attenuation and system settings (e.g., gain) [18]. Additional developments are needed to implement quick and quantitative readouts, ideally in realtime, on clinical systems to facilitate clinical translation of ultrasound molecular imaging.

Potential Clinical Applications

Inflammation Imaging with Ultrasound Molecular Imaging—Inflammation is part of the biological response of the body to a broad spectrum of stimuli, including toxins, ischemia, pathogens, etc. [4]. One of the hallmarks of inflammation and part of the cellular response of the body to those stimuli is the recruitment of inflammatory cells including leukocytes into the inflamed tissue. For leukocytes to transmigrate from the blood circulation into inflamed tissue, they need to first firmly adhere to the vascular endothelial cell wall. This process of leukocyte extravasation is receptor-mediated through various adhesion molecules expressed on the vessel wall including selectins (P-, E, and L-selectins), and immunoglobulin ligands ICAM1 and VCAM1. Leukocytes express ligands on their cell membrane that interact with those adhesion molecules, thereby allowing them first to roll and then firmly attach to the vessel wall [4]. This natural pathway of leukocyte rolling and attachment has been leveraged for ultrasound molecular imaging by designing microbubbles that can attach to adhesion markers serving as biomarkers of inflammation. Inflammation is a critical part of multiple disease processes and ultrasound molecular imaging of inflammation has been successfully shown for several disease processes including inflammatory bowel disease (Figure 3), myocardial ischemia, atherosclerosis, and rejection in cardiac transplantation (Table 1).

Imaging Inflammation in Inflammatory Bowel Disease—Inflammatory bowel disease is a chronic recurrent and complex group of diseases, including Crohn's disease and ulcerative colitis, that affects approximately 1.4 million patients in North America and that share similar pathology including infiltration of leukocytes, production of inflammatory mediators, and tissue remodeling that ultimately leads to ulcerations and bowel injury [19]. Accurate monitoring of disease activity to optimize therapeutic interventions with minimal side effects is one of the greatest challenges for appropriate clinical management of IBD. Since ultrasound is widely accessible, relatively inexpensive, and does not involve ionizing radiation ultrasound molecular imaging may become a complementary management tool, in patients with known IBD, by accurately quantifying inflammation at the molecular level at known sites of inflammation (as assessed for example by endoscopy, CT, or MRI). This may allow better individualization of treatment regimens by earlier identification of non-responders from responders and by minimizing drug doses in patients responding to a certain treatment regimen [14, 19, 20].

Recently, a novel clinically translatable dual-selectin targeted microbubble has been introduced [21] which was functionalized to attach to both P- and E-selectin by covalently coupling a truncated human selectin-binding glycoprotein ligand 1 (PSGL1) fused to a human fragment crystallizable (or Fc) domain onto lipid-shelled microbubbles [21, 22]. Leveraging the natural pathway of leukocyte rolling on inflamed vascular endothelial cells, this contrast agent allowed accurate quantification of inflammation in a chemically-induced murine model of acute colitis (Figure 3). Furthermore, in an intra-animal cross-modality comparison study, dual-selectin targeted ultrasound molecular imaging signal correlated well with FDG uptake on PET-CT scans in murine colitis (Figure 3) [22]. As a further step towards clinical translation, Wang et al. showed feasibility and good reproducibility of ultrasound molecular imaging using this new contrast agent in a porcine acute terminal

ileitis model using a clinical ultrasound system (Figure 3) [14]. Furthermore, the magnitude of *in vivo* ultrasound imaging signal correlated well with *ex vivo* histology over a spectrum of inflammation grades ranging from normal to mild, moderate, and severe inflammation [23], suggesting that dual-selectin targeted ultrasound imaging may allow non-invasive and objective quantification of tissue inflammation at the molecular level in a large animal model. Further clinical developments of this contrast agent along with clinical trials are warranted to assess its potential to quantify and monitor inflammation in patients.

Imaging Ischemic Memory in the Myocardium—Current non-invasive diagnostic tests for patients with suspected acute coronary syndrome include a combination of ECG and serologic markers (e.g., troponin, creatine kinase). In certain populations, abnormalities can be non-specific for both ECG (e.g. left bundle branch block) and/or serologic markers (e.g. in patients with severe renal disease) [24]. Evaluation of left ventricular function and myocardial perfusion by contrast echocardiography is particularly useful in those with a non-diagnostic initial ECG [24]. However, this approach is less useful in patients with prior ischemic events who have pre-existing abnormalities, or in patients who are seen several hours after resolution of ischemia in whom perfusion and wall motion have returned to normal [24]. Detecting molecular alterations that persist for hours after ischemic injury may be helpful to spatially localize and detect recent but resolved myocardial ischemia independent of abnormalities in perfusion or wall motion.

For this potential clinical application, P-selectin has been studied as a molecular imaging target since it is stored in secretory vesicles (called Weibel-Palade bodies) and, after acute activation in response to even mild ischemia, is trafficked to the vascular endothelial cell surface within only a few minutes, persisting for hours after the ischemic injury (and following *de novo* synthesis and expression of P-selectin by the activated endothelial cells) [25]. It has been shown that in the post-ischemic myocardium, ultrasound molecular imaging signal substantially increased 3–10 fold using microbubbles targeted to P-selectin in mice [26] and rats [25] after transient myocardial ischemia. Using a non-human primate transient myocardial ischemia model, dual P- and E-selectin-targeted ultrasound of ischemic memory using the same contrast agent described above for IBD imaging has been recently translated from small to large animals with a $240\pm 85\%$ increase in the molecular imaging signal in ischemic myocardium compared to non-ischemic myocardium [27]. Since E-selectin expression is under transcriptional control and cell surface expression can be detected approximately two hours after acute stimulation [27], dual-targeting to both P- and E-selectin is advantageous as imaging signal can be detected from a few minutes up to several hours after the ischemic event. Future clinical trials following further clinical development of this contrast agent are expected to assess the value of selectin-targeted ultrasound imaging in the detection and managing of patients with for example atypical chest pain.

Imaging Inflammation in Atherosclerosis—Atherosclerosis is a complex disease process that often progresses over decades before becoming clinically evident. Assessing the risk for this disease in an individual without known disease relies on the detection of early events such as oxidative stress, lipid accumulation, or upregulation of endothelial cell

adhesion molecules that participate in leukocyte recruitment [24]. Imaging of endothelial cell adhesion molecules has been successfully demonstrated using ultrasound molecular imaging (Table 1). In preclinical murine models, ultrasound molecular imaging of ICAM-1, VCAM-1, and P-selectin has been shown to result in robust signal enhancement at sites of arteriosclerotic plaque development and has been used to detect the earliest stages of the disease prior to advanced atherosclerotic plaque developments [24, 28]. Similarly, Masseau and colleagues showed that VCAM-1-targeted microbubbles can be used to monitor vascular inflammation in a hypercholesterolemic swine model [29]. This study provided strong evidence that the effect of therapeutic interventions on the inflammatory status of the endothelium can be longitudinally monitored using ultrasound. Furthermore, since inflammation and diabetes mellitus are interwoven processes that potentiate each other and can lead to accelerated atherosclerosis, a model of diet induced obesity in macaque monkeys was used to define the role of inflammatory mediators such as P-selectin and VCAM-1 using ultrasound molecular imaging in a high-risk pro-atherosclerotic phenotype that mimics the human conditions of obesity and insulin resistance [30]. It has been shown that molecular imaging signal for both P-selectin and VCAM-1 increased (~2 fold) progressively over baseline after high fat diet was initiated by 4 months for P-selectin and by 8 months for VCAM-1. In contrast, insulin resistance progressively increased (5–7 fold) over the 2 year period. Endothelial expression of adhesion molecules occurred before any detectable changes in carotid intima-medial thickness and did not directly correlate with systemic markers of inflammation such as C-reactive protein. These data indicate that endothelial expression of adhesion molecules involved in atherogenesis is one of the early events in the development of diet induced obesity and insulin resistance. Ultrasound molecular imaging of the endothelial adhesion molecules can provide an early indication of proatherosclerotic phenotype long before changes in morphology can be detected [30].

Oncological Imaging with Ultrasound Molecular Imaging—Ultrasound molecular imaging may also play a major role in the field of cancer imaging by contributing to earlier detection, molecular profiling of cancer, better characterization of focal lesions, and treatment monitoring [31]. Neoangiogenesis, the formation and recruitment of new blood vessels from the host surrounding tissue, is one of the hallmarks of cancer and occurs very early in the tumor development. Several biomarkers that are differentially expressed on the vascular endothelial cells of cancer have been studied to evaluate the feasibility of tumor detection at early stages using ultrasound molecular imaging [32–34]. Most commonly studied biomarkers include well characterized molecular markers such as VEGFR2, $\alpha_v\beta_3$ integrin, and endoglin (Table 2). Microbubbles against VEGFR2 and endoglin were also successfully used to monitor the effects of anti-angiogenic drugs and chemotherapeutic agents [8, 35].

The aforementioned first clinical grade molecularly-targeted ultrasound contrast agent BR55, targeted against human VEGFR2, has been designed for cancer imaging and showed promising results in multiple preclinical murine models (subcutaneous xenograft and orthotopic models) of cancer including breast, colon, prostate and liver [8, 36–38]. Recently, this clinical grade contrast agent has enabled assessment of tumor progression in various transgenic mouse models that resemble tumor progression in patients (Figure 4) [32–34].

Pysz *et al.* showed that VEGFR2-targeted ultrasound imaging with BR55 can visualize down to sub-millimeter sized foci of pancreatic cancer in a transgenic mouse model (Pdx1-Cre, KRas^{G12D}, Ink4a^{-/-}) and the *in vivo* targeted ultrasound imaging signal was ~30 fold higher in tumors compared to control normal pancreatic tissue, indicating that ultrasonic molecular imaging could be used for earlier pancreatic cancer detection in a screening setting of high risk patients [33]. Besides differentiating normal from cancer tissue, ultrasound molecular imaging using BR55 has been shown to assess breast cancer progression in a transgenic mouse model of breast cancer (FVB/N-Tg(MMTV-PyMT)634Mul) [32]. *In vivo* imaging signal significantly increased as the mammary gland tissue progressed from normal to hyperplasia, ductal carcinoma *in situ* (precursor lesions) and invasive breast cancer due to an increase in the number of tumor vessels and the magnitude of VEGFR2 expression levels per tumor vessel. Furthermore, BR55 enabled differentiation of healthy and dysplastic liver tissue due to elevated VEGFR2 expression levels in dysplastic nodules in a hepatocyte-specific nuclear factor- κ B essential modulator (NEMO/I κ B kinase γ [IKK γ]) knock-out model of dysplasia which eventually progresses to hepatocellular carcinoma [34]. The study showed that BR55 may be used to detect dysplastic lesions in which non-targeted ultrasound contrast agents such as SonoVue® do not provide characteristic ultrasound enhancement pattern [34].

In addition to the more general neoangiogenesis markers such as VEGFR2, cancer specific molecular markers differentially expressed on the neovasculature of various cancer types have been discovered through techniques like DNA microarray analysis, mass spectrometry, proteomic analysis and were subsequently validated through immunohistochemical analyses in human tissues [39, 40]. Thymocyte differentiating antigen 1 (Thy1) and B7-H3 (CD276, a member of B7 family of immunomodulators) are two such novel markers that have been recently identified and validated as specific, differentially expressed potential vascular targets for ultrasound imaging of pancreatic cancer, ovarian, and breast cancer [39–41].

Ultrasound is already among the first line imaging modalities for organs such as the mammary glands, ovaries, liver and pancreas (in patients with appropriate acoustic window). It can therefore be envisioned to eventually integrate an ultrasound-based molecular imaging approach for earlier detection, characterization and treatment monitoring of these cancers in the clinic.

Clinical Translation of Ultrasound Molecular Imaging—Following extensive validation in various preclinical animal models and formal preclinical toxicity studies in different species, BR55, the first and currently only clinical grade molecularly-targeted ultrasound contrast agent, has been moved into early phase clinical trials in Europe and the USA for cancer imaging. At the University Hospital Amsterdam, safety of BR55 in humans and first proof-of-concept evidence that detectable levels of contrast binding to VEGFR2 can be reached in patients with prostate cancer have been assessed (ClinicalTrials.gov identifier: NCT01253213, Figure 4). An ongoing clinical trial in patients with prostate cancer at Stanford University is exploring feasibility and efficacy of volumetric VEGFR2-targeted ultrasound imaging with BR55 for prostate cancer detection prior to radical prostatectomy (ClinicalTrials.gov identifier: NCT02142608), using histology as reference standard. Furthermore, at the Catholic University of Rome, feasibility and efficacy of

VEGFR2-targeted ultrasound imaging with BR55 in patients with suspected ovarian and breast cancer is being explored, using post-surgical or post-biopsy histology as reference standard (European Union ClinicalTrials identifier: 2012-000699-40). Different doses of the contrast agent are administered to explore optimal dosing of BR55 for detecting VEGFR2 binding in various cancer types.

These first in-human proof of concept feasibility studies will stimulate further developments and refinement of this promising imaging technique and explore and validate novel clinical niche applications where the strength of ultrasound combined with molecular imaging capabilities can be leveraged.

Challenges and Future Directions—One of the main challenges for clinical ultrasound molecular imaging, like for any other molecular contrast agent, is the lengthy and expensive developmental cost because molecular imaging agents are treated as any other drug by regulatory authorities. While for PET agents, considered to be injected in “trace amounts”, an exploratory investigative new drug application (eIND) pathway is available in the USA which expedites early first-in-human phase 0 clinical trials with less requirements for preclinical animal testing and the opportunity to render go-no go decisions faster [42, 43], this pathway currently does not exist for other types of contrast agents such as contrast microbubbles. However, it is conceivable that regulatory agencies becoming more familiar with a certain contrast agent (e.g., a targeted microbubble with a certain chemical composition), may expedite clinical translation if only binding ligands for molecular targeting were exchanged. For example, peptide binding ligands with a fixed backbone and only a small variable domain [44] may lend themselves for this purpose because new contrast agents may only vary minimally.

Also, preclinical ultrasound molecular imaging has most commonly been performed in two-dimensions (2D) which allows sampling of a small anatomical area only. Emerging techniques are being developed to allow three-dimensional (3D) ultrasound molecular imaging [45, 46]. Recently, a new clinical matrix array transducer containing 9212 elements with an integrated microbeamformer was assessed for monitoring anti-angiogenic therapy with volumetric ultrasound molecular imaging in a preclinical human colon cancer xenograft model [45]. The transducer electronically steers the ultrasound beam over the entire tumor volume, allowing imaging and quantifying ultrasound molecular imaging signal at relatively high spatial resolution and nearly constant voxel resolution in the entire imaging volume [45]. Since tumors are heterogeneous due to hemorrhage and areas of necrosis with spatially varying vascularity and neoangiogenesis leading to possible sampling errors on 2D imaging, 3D capabilities of ultrasound molecular imaging are critically needed should it be developed for e.g. longitudinal disease monitoring in cancer. In fact, anti-angiogenic treatment effects were overestimated up to 73% on 2D compared to 3D ultrasound molecular imaging in human colon cancer xenografts [45].

CONCLUSION

Ultrasound molecular imaging has come a long way from first *in vitro* and *in vivo* preclinical concept studies to first in human clinical trials. Particularly, the safe and

convenient use of ultrasound makes it a very appealing imaging modality for certain clinical niche applications where a whole body imaging approach is not required. Imaging neoangiogenesis for earlier cancer detection and assessment of expression levels of adhesion molecules to visualize myocardial ischemic memory in patients with atypical chest pain or to monitor disease activity in patients with acute bouts of IBD are promising potential future clinical applications for ultrasound molecular imaging and are currently explored in small as well as large animal models as next critical steps towards clinical translation. Recent experiences with first in human testing of a new clinical grade molecularly targeted contrast agent in cancer will further support the development and refinement of ultrasound molecular imaging for clinical applications.

Acknowledgments

Grant support: Supported by the NIH R01DK092509-01A1 grant (JKW), NIH R01 CA155289-01A1 grant (JKW), and the Mildred Scheel Foundation for Cancer Research (LAE)

REFERENCES

1. Wilson SR, Burns PN. Microbubble-enhanced US in body imaging: what role? *Radiology*. 2010; 257(1):24–39. [PubMed: 20851938]
2. Pysz MA, Willmann JK. Targeted contrast-enhanced ultrasound: an emerging technology in abdominal and pelvic imaging. *Gastroenterology*. 2011; 140(3):785–790. [PubMed: 2125573]
3. Kiessling F, Fokong S, Bzyl J, Lederle W, Palmowski M, Lammers T. Recent advances in molecular, multimodal and theranostic ultrasound imaging. *Adv Drug Deliv Rev*. 2014; 72:15–27. [PubMed: 24316070]
4. Deshpande N, Needles A, Willmann JK. Molecular ultrasound imaging: current status and future directions. *Clin Radiol*. 2010; 65(7):567–581. [PubMed: 20541656]
5. Klibanov AL. Ligand-carrying gas-filled microbubbles: ultrasound contrast agents for targeted molecular imaging. *Bioconjug Chem*. 2005; 16(1):9–17. [PubMed: 15656569]
6. Pochon S, Tardy I, Bussat P, et al. BR55: a lipopeptide-based VEGFR2-targeted ultrasound contrast agent for molecular imaging of angiogenesis. *Invest Radiol*. 2010; 45(2):89–95. [PubMed: 20027118]
7. Kaneko OF, Willmann JK. Ultrasound for molecular imaging and therapy in cancer. *Quant Imaging Med Surg*. 2012; 2(2):87–97. [PubMed: 23061039]
8. Pysz MA, Foygel K, Rosenberg J, Gambhir SS, Schneider M, Willmann JK. Antiangiogenic cancer therapy: monitoring with molecular US and a clinically translatable contrast agent (BR55). *Radiology*. 2010; 256(2):519–527. [PubMed: 20515975]
9. Walday P, Tolleshaug H, Gjoen T, et al. Biodistributions of air-filled albumin microspheres in rats and pigs. *Biochem J*. 1994; 299(Pt 2):437–443. [PubMed: 8172604]
10. Willmann JK, Cheng Z, Davis C, et al. Targeted microbubbles for imaging tumor angiogenesis: assessment of whole-body biodistribution with dynamic micro-PET in mice. *Radiology*. 2008; 249(1):212–219. [PubMed: 18695212]
11. Kircher MF, Willmann JK. Molecular body imaging: MR imaging, CT, US. part I. principles. *Radiology*. 2012; 263(3):633–643. [PubMed: 22623690]
12. Klibanov AL, Rasche PT, Hughes MS, et al. Detection of individual microbubbles of ultrasound contrast agents: imaging of free-floating and targeted bubbles. *Invest Radiol*. 2004; 39(3):187–195. [PubMed: 15076011]
13. Willmann JK, Paulmurugan R, Chen K, et al. US imaging of tumor angiogenesis with microbubbles targeted to vascular endothelial growth factor receptor type 2 in mice. *Radiology*. 2008; 246(2):508–518. [PubMed: 18180339]
14. Wang H, Felt S, Machtaler S, et al. Ultrasound Molecular Imaging of Inflammation in a Porcine Acute Terminal Ileitis Model. *Radiology*. 2015 In press.

15. Wang DS, Panje C, Pysz MA, et al. Cationic versus neutral microbubbles for ultrasound-mediated gene delivery in cancer. *Radiology*. 2012; 264(3):721–732. [PubMed: 22723497]
16. Panje CM, Wang DS, Willmann JK. Ultrasound and microbubble-mediated gene delivery in cancer: progress and perspectives. *Invest Radiol*. 2013; 48(11):755–769. [PubMed: 23697924]
17. Pysz MA, Guracar I, Tian L, Willmann JK. Fast microbubble dwell-time based ultrasonic molecular imaging approach for quantification and monitoring of angiogenesis in cancer. *Quant Imaging Med Surg*. 2012; 2(2):68–80. [PubMed: 22943043]
18. Wang S, Mauldin FW Jr, Klibanov AL, Hossack JA. Ultrasound-based measurement of molecular marker concentration in large blood vessels: a feasibility study. *Ultrasound Med Biol*. 2015; 41(1):222–234. [PubMed: 25308943]
19. Deshpande N, Lutz AM, Ren Y, et al. Quantification and monitoring of inflammation in murine inflammatory bowel disease with targeted contrast-enhanced US. *Radiology*. 2012; 262(1):172–180. [PubMed: 22056689]
20. Bachmann C, Klibanov AL, Olson TS, et al. Targeting mucosal addressin cellular adhesion molecule (MAdCAM)-1 to noninvasively image experimental Crohn's disease. *Gastroenterology*. 2006; 130(1):8–16. [PubMed: 16401463]
21. Bettinger T, Bussat P, Tardy I, et al. Ultrasound molecular imaging contrast agent binding to both E- and P-selectin in different species. *Invest Radiol*. 2012; 47(9):516–523. [PubMed: 22814589]
22. Wang H, Machtaler S, Bettinger T, et al. Molecular imaging of inflammation in inflammatory bowel disease with a clinically translatable dual-selectin-targeted US contrast agent: comparison with FDG PET/CT in a mouse model. *Radiology*. 2013; 267(3):818–829. [PubMed: 23371306]
23. Wei K, Main ML, Lang RM, et al. The effect of Definity on systemic and pulmonary hemodynamics in patients. *J Am Soc Echocardiogr*. 2012; 25(5):584–588. [PubMed: 22365709]
24. Inaba Y, Lindner JR. Molecular imaging of disease with targeted contrast ultrasound imaging. *Transl Res*. 2012; 159(3):140–148. [PubMed: 22340763]
25. Hyvelin JM, Tardy I, Bettinger T, et al. Ultrasound molecular imaging of transient acute myocardial ischemia with a clinically translatable P- and E-selectin targeted contrast agent: correlation with the expression of selectins. *Invest Radiol*. 2014; 49(4):224–235. [PubMed: 24442162]
26. Kaufmann BA, Lewis C, Xie A, Mirza-Mohd A, Lindner JR. Detection of recent myocardial ischaemia by molecular imaging of P-selectin with targeted contrast echocardiography. *Eur Heart J*. 2007; 28(16):2011–2017. [PubMed: 17526905]
27. Davidson BP, Chadderdon SM, Belcik JT, Gupta S, Lindner JR. Ischemic memory imaging in nonhuman primates with echocardiographic molecular imaging of selectin expression. *J Am Soc Echocardiogr*. 2014; 27(7):786–793. e2. [PubMed: 24774222]
28. Kaufmann BA, Carr CL, Belcik JT, et al. Molecular imaging of the initial inflammatory response in atherosclerosis: implications for early detection of disease. *Arterioscler Thromb Vasc Biol*. 2010; 30(1):54–59. [PubMed: 19834105]
29. Masseau I, Davis MJ, Bowles DK. Carotid inflammation is unaltered by exercise in hypercholesterolemic Swine. *Med Sci Sports Exerc*. 2012; 44(12):2277–2289. [PubMed: 22776877]
30. Chadderdon SM, Belcik JT, Bader L, et al. Proinflammatory endothelial activation detected by molecular imaging in obese nonhuman primates coincides with onset of insulin resistance and progressively increases with duration of insulin resistance. *Circulation*. 2014; 129(4):471–478. [PubMed: 24163066]
31. Deshpande N, Pysz MA, Willmann JK. Molecular ultrasound assessment of tumor angiogenesis. *Angiogenesis*. 2010; 13(2):175–188. [PubMed: 20549555]
32. Bachawal SV, Jensen KC, Lutz AM, et al. Earlier detection of breast cancer with ultrasound molecular imaging in a transgenic mouse model. *Cancer Res*. 2013; 73(6):1689–1698. [PubMed: 23328585]
33. Pysz MA, Machtaler SB, Seeley ES, et al. Vascular endothelial growth factor receptor type 2-targeted contrast-enhanced US of pancreatic cancer neovasculature in a genetically engineered mouse model: potential for earlier detection. *Radiology*. 2015; 274(3):790–799. [PubMed: 25322341]

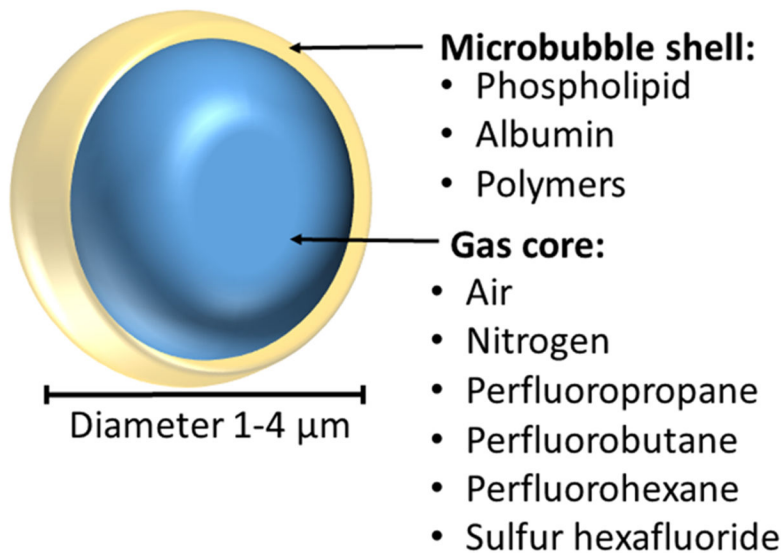
34. Grouls C, Hatting M, Rix A, et al. Liver dysplasia: US molecular imaging with targeted contrast agent enables early assessment. *Radiology*. 2013; 267(2):487–495. [PubMed: 23360735]
35. Leguerney I, Scoazec JY, Gadot N, et al. Molecular ultrasound imaging using contrast agents targeting endoglin, vascular endothelial growth factor receptor 2 and integrin. *Ultrasound Med Biol*. 2015; 41(1):197–207. [PubMed: 25308938]
36. Bzyl J, Lederle W, Rix A, et al. Molecular and functional ultrasound imaging in differently aggressive breast cancer xenografts using two novel ultrasound contrast agents (BR55 and BR38). *Eur Radiol*. 2011; 21(9):1988–1995. [PubMed: 21562807]
37. Sugimoto K, Moriyasu F, Negishi Y, et al. Quantification in molecular ultrasound imaging: a comparative study in mice between healthy liver and a human hepatocellular carcinoma xenograft. *J Ultrasound Med*. 2012; 31(12):1909–1916. [PubMed: 23197543]
38. Tardy I, Pochon S, Theraulaz M, et al. Ultrasound molecular imaging of VEGFR2 in a rat prostate tumor model using BR55. *Invest Radiol*. 2010; 45(10):573–578. [PubMed: 20808233]
39. Bachawal SV, Jensen KC, Wilson KE, et al. Breast Cancer Detection by B7-H3 Targeted Ultrasound Molecular Imaging. *Cancer Res*. 2015 In press.
40. Foygel K, Wang H, Machtaler S, et al. Detection of pancreatic ductal adenocarcinoma in mice by ultrasound imaging of thymocyte differentiation antigen 1. *Gastroenterology*. 2013; 145(4):885–894. e3. [PubMed: 23791701]
41. Lutz AM, Bachawal SV, Drescher CW, Pysz MA, Willmann JK, Gambhir SS. Ultrasound molecular imaging in a human CD276 expression-modulated murine ovarian cancer model. *Clin Cancer Res*. 2014; 20(5):1313–1322. [PubMed: 24389327]
42. Mosessian S, Duarte-Vogel SM, Stout DB, et al. INDs for PET molecular imaging probes—approach by an academic institution. *Mol Imaging Biol*. 2014; 16(4):441–448. [PubMed: 24733693]
43. Kircher MF, Willmann JK. Molecular body imaging: MR imaging, CT, US. Part II. Applications. *Radiology*. 2012; 264(2):349–368. [PubMed: 22821695]
44. Willmann JK, Kimura RH, Deshpande N, Lutz AM, Cochran JR, Gambhir SS. Targeted contrast-enhanced ultrasound imaging of tumor angiogenesis with contrast microbubbles conjugated to integrin-binding knottin peptides. *J Nucl Med*. 2010; 51(3):433–440. [PubMed: 20150258]
45. Wang H, Kaneko OF, Tian L, Hristov D, Willmann JK. Three-Dimensional Ultrasound Molecular Imaging of Angiogenesis in Colon Cancer Using a Clinical Matrix Array Ultrasound Transducer. *Invest Radiol*. 2015
46. Streeter JE, Gessner RC, Tsuruta J, Feingold S, Dayton PA. Assessment of molecular imaging of angiogenesis with three-dimensional ultrasonography. *Mol Imaging*. 2011; 10(6):460–468. [PubMed: 22201537]
47. Tranquart F, Arditi M, Bettinger T, et al. Ultrasound Contrast Agents For Ultrasound Molecular Imaging. *Z Gastroenterol*. 2014; 52(11):1268–1276. [PubMed: 25390214]
48. Davidson BP, Kaufmann BA, Belcik JT, Xie A, Qi Y, Lindner JR. Detection of antecedent myocardial ischemia with multiselectin molecular imaging. *J Am Coll Cardiol*. 2012; 60(17):1690–1697. [PubMed: 23021335]
49. Leng X, Wang J, Carson A, et al. Ultrasound detection of myocardial ischemic memory using an E-selectin targeting peptide amenable to human application. *Mol Imaging*. 2014; 13:1–9. [PubMed: 24824960]
50. Hamilton AJ, Huang SL, Warnick D, et al. Intravascular ultrasound molecular imaging of atheroma components in vivo. *J Am Coll Cardiol*. 2004; 43(3):453–460. [PubMed: 15013130]
51. Khanicheh E, Qi Y, Xie A, et al. Molecular imaging reveals rapid reduction of endothelial activation in early atherosclerosis with apocynin independent of antioxidative properties. *Arterioscler Thromb Vasc Biol*. 2013; 33(9):2187–2192. [PubMed: 23908248]
52. Weller GE, Lu E, Csikari MM, et al. Ultrasound imaging of acute cardiac transplant rejection with microbubbles targeted to intercellular adhesion molecule-1. *Circulation*. 2003; 108(2):218–224. [PubMed: 12835214]
53. Korpanty G, Carbon JG, Grayburn PA, Fleming JB, Brekken RA. Monitoring response to anticancer therapy by targeting microbubbles to tumor vasculature. *Clin Cancer Res*. 2007; 13(1):323–330. [PubMed: 17200371]

54. Willmann JK, Lutz AM, Paulmurugan R, et al. Dual-targeted contrast agent for US assessment of tumor angiogenesis in vivo. *Radiology*. 2008; 248(3):936–944. [PubMed: 18710985]
55. Deshpande N, Ren Y, Foygel K, Rosenberg J, Willmann JK. Tumor angiogenic marker expression levels during tumor growth: longitudinal assessment with molecularly targeted microbubbles and US imaging. *Radiology*. 2011; 258(3):804–811. [PubMed: 21339349]
56. Barua A, Yellapa A, Bahr JM, et al. VEGFR2-Targeted Ultrasound Imaging Agent Enhances the Detection of Ovarian Tumors at Early Stage in Laying Hens, a Preclinical Model of Spontaneous Ovarian Cancer. *Ultrasound Imaging*. 2014
57. Frinking PJ, Tardy I, Theraulaz M, et al. Effects of acoustic radiation force on the binding efficiency of BR55, a VEGFR2-specific ultrasound contrast agent. *Ultrasound Med Biol*. 2012; 38(8):1460–1469. [PubMed: 22579540]
58. Wei S, Fu N, Sun Y, et al. Targeted contrast-enhanced ultrasound imaging of angiogenesis in an orthotopic mouse tumor model of renal carcinoma. *Ultrasound Med Biol*. 2014; 40(6):1250–1259. [PubMed: 24613557]
59. Ellegala DB, Leong-Poi H, Carpenter JE, et al. Imaging tumor angiogenesis with contrast ultrasound and microbubbles targeted to alpha(v)beta3. *Circulation*. 2003; 108(3):336–341. [PubMed: 12835208]
60. Barua A, Yellapa A, Bahr JM, et al. Enhancement of ovarian tumor detection with alphavbeta3 integrin-targeted ultrasound molecular imaging agent in laying hens: a preclinical model of spontaneous ovarian cancer. *Int J Gynecol Cancer*. 2014; 24(1):19–28. [PubMed: 24304684]
61. Anderson CR, Hu X, Zhang H, et al. Ultrasound molecular imaging of tumor angiogenesis with an integrin targeted microbubble contrast agent. *Invest Radiol*. 2011; 46(4):215–224. [PubMed: 21343825]
62. Warram JM, Sorace AG, Saini R, Umphrey HR, Zinn KR, Hoyt K. A triple-targeted ultrasound contrast agent provides improved localization to tumor vasculature. *J Ultrasound Med*. 2011; 30(7):921–931. [PubMed: 21705725]
63. Sorace AG, Saini R, Mahoney M, Hoyt K. Molecular ultrasound imaging using a targeted contrast agent for assessing early tumor response to antiangiogenic therapy. *J Ultrasound Med*. 2012; 31(10):1543–1550. [PubMed: 23011617]
64. Sanna V, Pintus G, Bandiera P, et al. Development of polymeric microbubbles targeted to prostate-specific membrane antigen as prototype of novel ultrasound contrast agents. *Mol Pharm*. 2011; 8(3):748–757. [PubMed: 21545176]
65. Wang L, Li L, Guo Y, et al. Construction and in vitro/in vivo targeting of PSMA-targeted nanoscale microbubbles in prostate cancer. *Prostate*. 2013; 73(11):1147–1158. [PubMed: 23532872]
66. Tsuruta JK, Klauber-DeMore N, Streeter J, et al. Ultrasound molecular imaging of secreted frizzled related protein-2 expression in murine angiosarcoma. *PLoS One*. 2014; 9(1):e86642. [PubMed: 24489757]

Highlights

- Ultrasound molecular imaging is a highly sensitive modality.
- A clinical grade ultrasound contrast agent has entered first in human clinical trials.
- Several new potential future clinical applications of ultrasound molecular imaging are being explored.

A



B

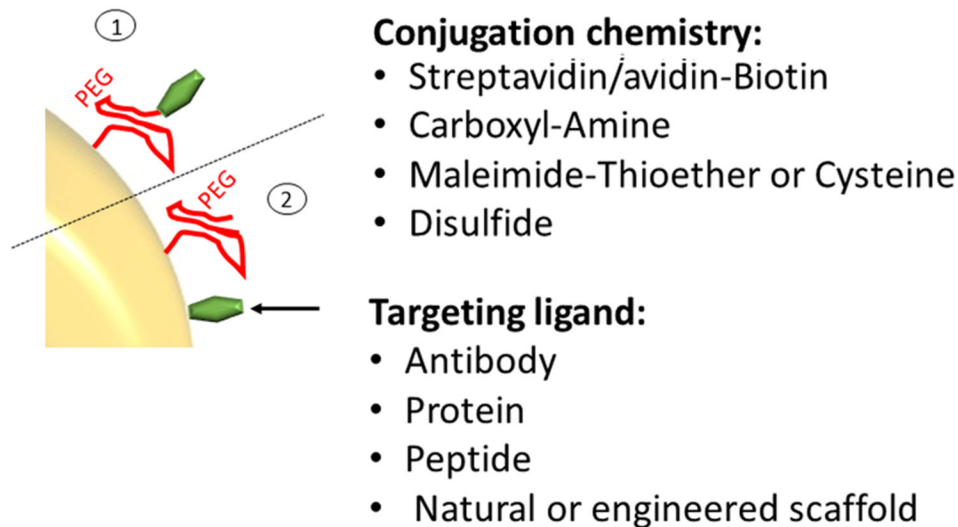


Figure 1. Design of molecularly-targeted microbubbles

(A) Microbubbles are 1–4 μm microspheres with a shell composed of various materials and a core that can contain different types of gases. (B) Incorporated PEG chains stabilize the microbubble shell, form a steric barrier to prevent coalescence, minimize adsorption of macromolecules to the microbubble surface, and provide spacing between the shell and binding ligands. Various types of ligands (e.g., antibodies, proteins, peptides) can be attached non-covalently or covalently by using biotin/streptavidin, biotin/avidin, amine

(NH₂)/amide, maleimide/thioether, 2-(Pridylthio)propionyl (PDP)/disulfide, either via the PEG arm (1) or directly onto the shell surface (2).

Author Manuscript

Author Manuscript

Author Manuscript

Author Manuscript

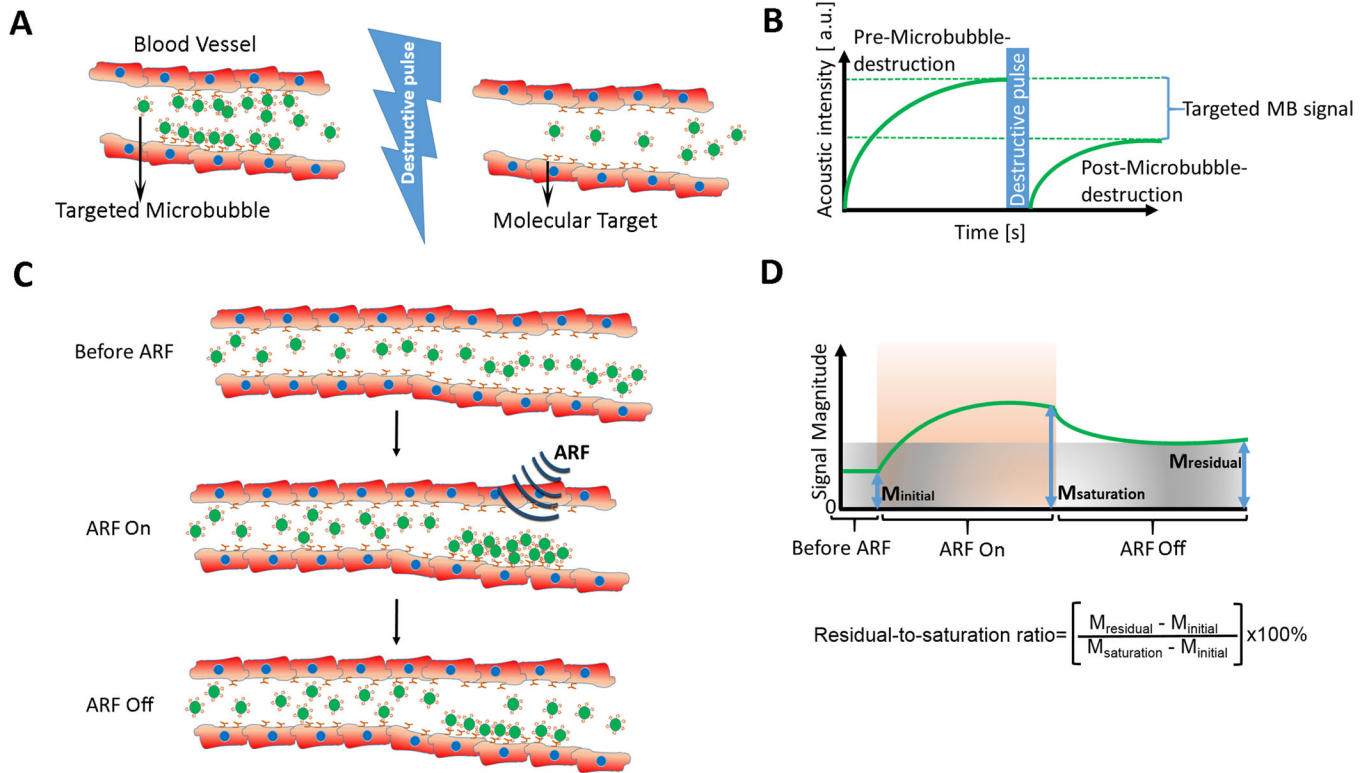


Figure 2. Examples of quantification techniques of ultrasound molecular imaging signal
 (A) Destruction-replenishment technique shown graphically in a vessel expressing molecular imaging targets (red) and after injection of molecularly-targeted microbubbles (green). (B) Imaging signal in field of view increases after intravenous injection of targeted microbubbles and is composed of signal from attached and freely circulating microbubbles as well as tissue background signal. After a few minutes, a high pressure destructive pulse destroys all microbubbles within the beam elevation and after an additional few seconds freely circulating microbubbles have replenished into the field of view. The difference in imaging signal pre and post destruction corresponds to the signal from attached microbubbles (targeted MB signal). Modified from [13]. (C) Assessment of the attenuation independent residual-to-saturation ratio using acoustic radiation force. After injection of molecularly-targeted microbubbles (green) an acoustic radiation force (ARF) pulse gently pushes targeted microbubbles to the vascular endothelial cell wall thereby enhancing molecular target attachment of microbubbles. After terminating the push pulse, unbound microbubbles are released due to flow shear forces and only firmly attaching microbubbles stay attached. (D) The initial signal M_{initial} represents the background signal of the tissue in the absence of adherent microbubbles. After ARF pulses, the imaging signal from locally accumulating microbubbles enhances up to full saturation ($M_{\text{saturation}}$). After termination of the ARF pulse, non-attached microbubbles float away and the imaging signal from attached microbubbles (M_{residual}) can be measured. Modified from [18].

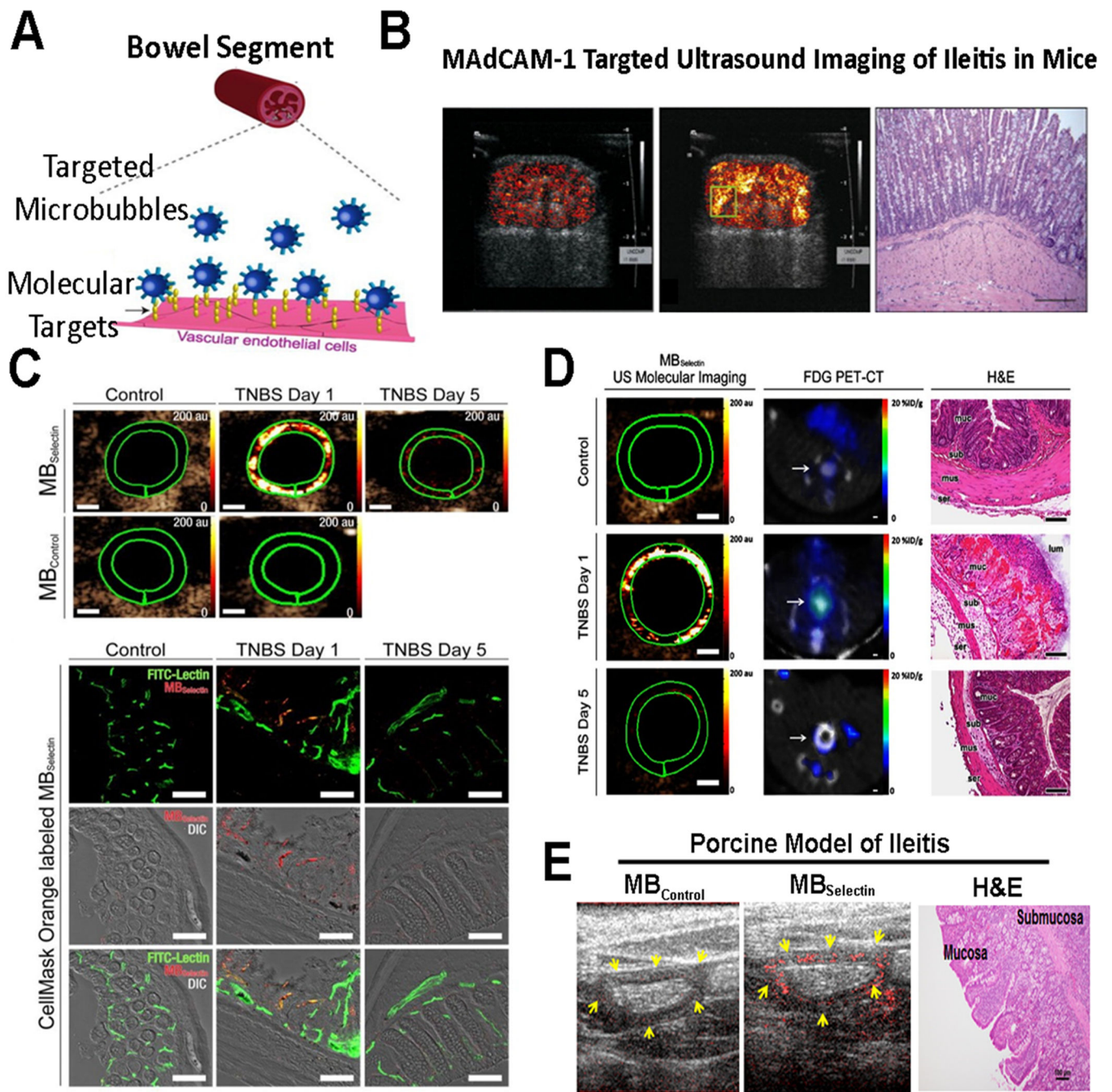


Figure 3. Molecular imaging of inflammation in inflammatory bowel disease
 (A) Schematic representation shows molecularly-targeted microbubbles (blue) binding to molecular markers expressed on the vascular endothelial cells of inflamed capillaries in a bowel segment. Modified from [22]. (B) Ultrasound molecular imaging of Mucosal Addressin Cellular Adhesion Molecule (MAdCAM-1) in an IBD model of spontaneous ileitis in mice shows weak background signal in non-inflamed ileum (left) and strong signal in acute ileitis (middle); histology confirms active inflammation (right). Reproduced with permission from [20]. (C) Transverse dual P- and E-selectin targeted ultrasound images

obtained in mice with chemically induced acute colitis scanned at day 1 (severe colitis), day 5 (mild colitis), and in mouse with normal colon, compared to imaging with control, non-targeted microbubbles. Note strong signal in acute inflammation at day 1 which decreases when inflammation is reduced at day 5 (scale bar = 1 mm). Representative confocal micrographs overlaid on differential interference contrast images show accumulation of fluorescently labeled selectin-targeted microbubbles (red) in mucosal capillaries (green) in acute inflammation but not in non-inflamed colon tissue (scale bar = 100 μ m). Reprinted with permission from [22]. (D) Cross-modality intra-animal comparison of dual-selectin-targeted ultrasound and FDG PET-CT imaging shows good quantitative correlation of both modalities (scale bar, 1 mm) with histology confirming imaging results. (E) Translational study in acute terminal ileitis model in a pig shows feasibility of dual-selectin targeted ultrasound imaging signal (middle) with substantially increased imaging signal compared to control non-targeted contrast agent (left) in inflamed ileum. Histology confirms inflammation (right).

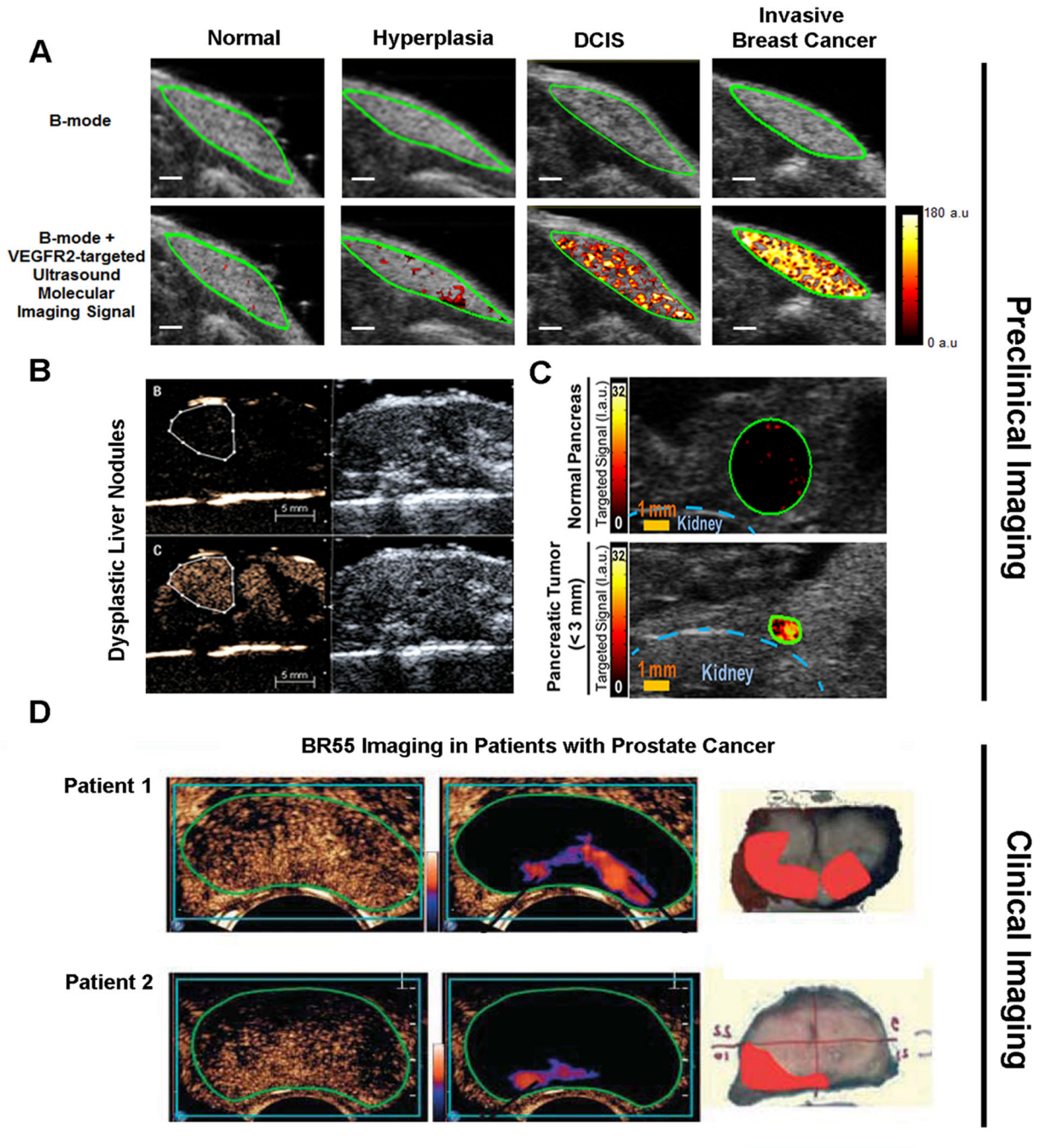


Figure 4. Preclinical and clinical examples of ultrasound molecular imaging of cancer and cancer development using clinical grade vascular endothelial cell receptor type 2 (VEGFR2) targeted microbubbles (BR55)

(A) Ultrasound molecular images using BR55 in transgenic mouse model of breast cancer development shows substantially increasing imaging signal in the mammary gland with breast tissue progressing from normal to hyperplasia, ductal carcinoma in situ, and invasive breast cancer, suggesting that the magnitude of imaging signal at the cancer stage may help earlier detection of breast cancer using ultrasound molecular imaging. Reprinted with permission from [32]. (B) In a transgenic mouse model of hepatocellular carcinoma

development, VEGFR2-targeted ultrasound imaging allowed diagnosing of dysplastic nodule based on magnitude of imaging signal (lower row) while non-targeted contrast-enhanced ultrasound imaging could not differentiate between healthy and dysplastic liver tissue. Reprinted with permission from [34]. (C) Ultrasound imaging also allows visualization of early pancreatic adenocarcinoma in a transgenic mouse model of spontaneous pancreatic cancer development with small foci of cancer showing substantially higher signal (lower row) than normal pancreatic tissue (upper row) due to strong expression of VEGFR2, suggesting that this technology could be used for screening purposes in high risk populations. Reprinted with permission from [33]. (D) Examples of transrectal transverse VEGFR2-targeted ultrasound molecular images in two patients with biopsy-proven prostate cancer, imaged 11 min following intravenous contrast agent injection. Raw data images (left, showing mixed signal from freely circulating and attached microbubbles) and post-processed images (middle; highlighting signal from stationary (attached) microbubbles) show foci of enhanced signal in the peripheral zone suggesting presence of cancer. Right images show corresponding macroscopy slices following radical prostatectomy with the extent of prostate cancer assessed by pathological analysis overlaid in red. Reprinted with permission from [47].

Table 1

Overview of Publications on Ultrasound Molecular Imaging of Inflammation in Various Diseases

Disease	Molecular Target	Animal Model	Reference
Inflammatory Bowel Disease	Mad-CAM-1	Mouse	Bachmann C, 2006 [20]
	P-selectin	Mouse	Deshpande N, 2012 [19]
	Dual selectin (P&E)	Mouse	Wang H, 2013 [22]
	Dual selectin (P&E)	Swine	Wang H, 2015 [14]
Myocardial Ischemia	P-selectin	Mouse	Kaufmann BA, 2007 [26]
	Dual Selectin (P&E)	Mouse	Davidson BP, 2012 [48]
	E-selectin	Rat	Leng X, 2014 [49]
	Dual Selectin (P&E)	Non-Human Primate	Davidson BP, 2014 [27]
	Dual Selectin (P&E)	Rat	Hyvelin JM, 2014 [25]
Atherosclerosis	VCAM-1 and ICAM-1	Swine	Hamilton AJ, 2004 [50]
	VCAM-1 and P-selectin	Mouse	Kauffmann BA, 2010 [28]
	VCAM-1	Mouse	Khanicheh E, 2013 [51]
	VCAM-1 and P-selectin	Non-Human Primates	Chadderdon SM, 2014 [30]
Cardiac Transplant Rejection	ICAM-1	Rat	Weller GE, 2003 [52]

Table 2

Overview of Publications on Ultrasound Molecular Imaging in Various Cancer Types

Molecular Target	Cancer Type	Reference
VEGFR2	Pancreatic	Korpanty G, 2007 [53]; Pysz MA, 2014 [33].
	Angiosarcoma	Willmann JK, 2008 [13]
	Ovarian	Willmann JK, 2008 [54]; Deshpande N 2011 [55], Barua A, 2014 [56]
	Prostate	Tardy I, 2010 [38]; Frinking PJ, 2012 [57]
	Breast	Deshpande N, 2011 [55], Byzl J, 2011 [36], Bachawal SV, 2013 [32]
	Colon	Pysz MA, 2012 [17]; Wang H, 2015 [45]
	Liver	Sugimoto K, 2012 [37]
	Renal	Wei S, 2014 [58]
	Integrin	Glioma
Ovarian		Willmann JK, 2008 [54]; Willmann JK, 2010 [44]; Deshpande N 2011 [55]; Barua A, 2014 [60]
Breast		Anderson CR 2011 [61]; Warram JM, 2011 [62]; Sorace AG, 2012 [63]
Endoglin/CD105	Pancreatic	Korpanty G, 2007 [53]
	Ovarian	Deshpande N, 2011 [55]
	Melanoma	Legurney I, 2015 [35]
Thy1/CD90	Pancreatic	Foygel K, 2013 [40]
B7-H3/CD276	Ovarian	Lutz AM, 2013 [41];
	Breast	Bachawal SV, 2015 [39]
PSMA	Prostate	Sanna V, 2011 [64]; Wang L, 2013 [65]
Secreted Frizzled Related Protein-2	Angiosarcoma	Tsuruta JK, 2014 [66]